Observation and theoretical modeling of electron scale solar sind turbulence

F. Sahraoui*
Laboratoire de Physique des Plasmas, CNRS-Ecole Polytechnique, Observatoire de Saint-Maur, 4 avenue de Nepture, 94107 Saint-Maur-des-Fossés, France

M. L. Goldstein
NASA Goddard Space Flight Center, Code 673, Greenbelt 20771, Maryland, USA

K. Abdul-Kader, G. Belmont, L. Rezeau,† P. Robert, and P. Canu
Laboratoire de Physique des Plasmas, CNRS-Ecole Polytechnique, Route de Sacaly, 91000 Palaiseau, France and Laboratoire de Physique des Plasmas, CNRS-Ecole Polytechnique, Route de Sacaly, 91000, Palaiseau France
(Dated: March 8, 2010)

Turbulence at MagnetoHydroDynamics (MHD) scales of the solar wind has been studied for more than three decades, using data analyzes, theoretical and numerical modeling. However smaller scales have not been explored until very recently. Here, we review recent results on the first observation of cascade and dissipation of the solar wind turbulence at the electron scales. Thanks to the high resolution magnetic and electric field data of the Cluster spacecraft, we computed the spectra of turbulence up to $\sim$ 100 Hz (in the spaceraft reference frame) and found evidence of energy dissipation around the Doppler-shifted electron gyroscale f_{ρ_e}. Before its dissipation, the energy is shown to undergo two cascades: a Kolmogorov-like cascade with a scaling $f^{-1.6}$ above the proton gyroscale, and a new $f^{-2.3}$ cascade at the sub-proton and electron gyroscales. Above f_{ρ_e} the spectrum has a steeper power law $\sim f^{-4.1}$ down to the noise level of the instrument. Solving numerically the linear Maxwell-Vlasov equations combined with recent theoretical predictions of the Gyro-Kinetic theory, we show that the present results are consistent with a scenario of a quasi-two-dimensional cascade into Kinetic Alfvén modes (KAW). New analyses of other data sets, where the Cluster separation ($\sim$ 100 km) allowed us to explore the sub-proton scales using the k-filtering technique, and to confirm the 2-D nature of the turbulence at those scales.

PACS numbers: Valid PACS appear here

I. INTRODUCTION

Over the past three decades, the solar wind (SW) has provided a unique "laboratory" to explore fundamentals of the plasma physics in general and turbulence in particular. Owing to the permanent plasma flow ejected by the solar corona, the solar wind shows fluctuations on all physical quantities (magnetic and electric fields, density, temperature, ...) and on all scales. Away form the Sun, the turbulence develops nearly freely from any bourdary and evolves under the sole nonlinear interactions taking place within the plasma. This makes the solar wind un ideal place to explore plasma turbulence, theoretically, numerically and observationally. Observations of the SW turbulence have been possible thanks in particular to the availability of the *in-situ* data measured by single spacecraft such as Voyager, Ulysses, and Wind, or multi-satellites like Cluster [1] and Themis. Mono-satellite data allow one to measure fluctuations only in the (temporal) angular frequency domain, while theories of turbulence predict generally (spatial) wave number properties. In the solar wind comparisons between observations and theories is made possible using the frozen-in flow approximation, known also as the Taylor hypothesis, $\omega_{sc} \sim \mathbf{k}.\mathbf{V}_f$, where ω_{sc} is the measured angular frequency in the spacecraft frame and $\mathbf{V}_f$ is the average flow speed. The solar wind being super-sonic and super-Alfvénic, this assumption is justified since all the characteristic low frequency (Alfvén and magnetosonic) waves have phase speeds smaller than V_f. However, the Taylor assumption is violated if high frequency waves, e.g., whistlers are present. It is also violated in other physical contexts, such as the magnetosphere, where all the characteristic speeds (V_f, V_A, C_S) are of the same order. It is worth noticing that even when the Taylor hypothesis is fully justified, one can infer the wave number properties only along the flow direction. The two other directions of space remain unresolved unless further assumption are introduced such us the isotropy of the turbulence. To fully solve the problem of the 3-D determination of the properties of the SW multi-spacecraft data, such us Cluster, and Themis are required.

Early observations of SW turbulence have emphasized magnetohydrodynamic (MHD) scales where the Kolmogovov scaling $k^{-5/3}$ is frequently observed [2], and usually explained by the energy cascade of nonlinearly interacting (inward and outward) Alfvén waves. This k-spectrum has been obtained so far using the Taylor hypothesis. Recently, and thanks to the availability of the Cluster multi-spacecraft data, and to the use of multi-

*Electronic address: fouad.sahraoui@lpp.polytechnique.fr
†Université Pierre et Marie Curie, UPMC, Place Jussieu, Paris, France

point measurements techniques such as the k-filtering (known also as the $wave - telescope$ technique), new results on the actual 3-D turbulence of MHD turbulence are being obtained [3, 4]. Here we focus only on the turbulence at frequencies above the proton gyrofrequency ($f_{cp} \sim 0.1$ Hz). Above f_{cp} and up to 10 Hz steeper power law spectra $f^{-\alpha}$ with $2 < \alpha < 4$ have been observed [5–8] and a debate exists as to whether the turbulence has become dispersive following the whistler mode or the KAW branch, before it is dissipated at small scales [9, 10].

There are several theoretical predictions on small scale turbulence: Biskamp et al. [11] predicted a $k^{-7/3}$ magnetic spectrum of whistler turbulence either by dimensional analyses *à la Kolmogorov* or numerical simulations. Later on, several author have confirmed those predictions [12, 13]. Recently, Galtier [14] has shown that the exact Yaglom's-type of equations he obtained for isotropic incompressible Hall-MHD (HMHD) turbulence allow one to derive the $k^{-7/3}$ scaling, which provides thus a stronger theoretical ground for the $k^{-7/3}$ spectrum. Weak turbulence theory of anisotropic incompressible HMHD predicts a ${k_\perp}^{-5/2}$ scaling for either the whistler or the Alfvén branches [12, 14, 15]. While all these fluid models are good approximations and provide important features of the SW turbulence, one has however to bear in mind their validity limits and the approximations that had been used to derive them from the exact kinetic theory. Such cautions are particularly required in studies of hot plasmas or scales where dissipations occur (e.g., proton or electron gyroscales). For such problems a kinetic theory is needed. But owing to the fact that a turbulence theory in the full-kinetic approximation is yet out-of-reach, simplified kinetic models may provide an alternative. Such theories exist, and one of them Gyro-Kinetics (GK). This theory has been developped in the seventies for studying confinement in fusion plasmas. In has been introduced only recently into space and astrophysical applications (see [16] where a review of the theory is given). By averaging over the fast motion of protons GK theory allows one to describe only the very slow dynamics of the plasma ($\omega << \omega_{cp}$). It assumes furthermore a strong anisotropy $k_\parallel << k_\perp$, allowing expansion of the equations on the small parameter $\epsilon = k_\parallel / k_\perp$, making thus the theorie mathematically tractable. Under these approximations, the classical fast (or whistler) mode is obviously ruled out. But, GK catches most of the physics of the Alfvén mode ($\omega \sim k_\parallel V_A$) and that of the entropy mode ($\omega = 0$) down to the electron scales ($k\rho_e \sim 1$). For the scales $1/\rho_e < L < 1/\rho_i$, amond others, KG preditcs the scalings ${k_\perp}^{-7/3}$ for the magnetic spectrum and ${k_\perp}^{-1/3}$ for the electric field spectrum [16, 17].

II. HIGH FREQUENCY CLUSTER DATA IN THE SOLAR WIND

In the present work, we analyze high frequencies (up to 100 Hz) of solar wind magnetic and electric turbulence by taking advantage of high resolution wave data from the Cluster spacecraft [1]. Magnetic data are from the Flux Gate Magnetometer (FGM) and the STAFF-Search Coil (SC) [18, 19] experiments, and electric field data are from the Electric Field and Wave experiment (EFW) [20]. FGM data cover the frequency spectrum up to a few Hz. STAFF-SC and EFW provide higher resolution data with two possible sampling rates: 25 Hz (normal mode) and 450 Hz (burst mode). The data used here are burst mode. Due to the small level of the magnetic turbulence in the SW at these very high frequencies, particular attention has been paid to several instrumental issues, in particular, the sensitivity of the STAFF-SC magnetometer. Because of the low sensitivity of the SC sensor at very low frequency, the lowest part of the STAFF-SC spectra has to be filtered. The cut-off frequency can be set to 0.35 Hz on the two perpendicular components to the spin axis. However, in this study, we filtered the spectra at 1.5 Hz to avoid any residual spin effect.

The waveforms shown on figure 1 were recorded on 19 March 2006 from 20h32 to 23h20 UT in the solar wind at 1 AU. During this period the Interplanetary Magnetic Field (IMF) was $B \sim 6$ nT, the plasma density $n_p \sim 3$ cm^{-3}, the proton and electron temperatures $T_p \sim 50$ eV and $T_e \sim 12$ eV, respectively, the plasma betas (ratios between thermal and magnetic pressures) $\beta_p \sim 2.5$ and $\beta_e \sim 0.7$, respectively for protons and electrons, the plasma velocity $v \sim 640$ km/s, the Alfvén speed $V_A \sim 65$ km/s and the proton gyrofrequency $f_{cp} \sim 0.1$ Hz. The plasma data (protons and electrons) have been obtained from the CIS and the PEACE experiments [1].

Figure 1 shows the magnetic field components measured by FGM. Note the rotations of B_y coincident with a minimum in the magnetic field magnitude, indicating possible multiple current sheet crossings as the spacecraft move from solar wind toward the bow shock. During this event reflected electrons from the bow shock have been observed both from the Peace and Whisper data. Figure 2 shows the power spectra of the magnetic field data from FGM and STAFF-SC, decomposed into the parallel and the perpendicular directions with respect to the mean IMF (defined by averaging over the time interval of Figure 1). These spectra are calculated using a windowed Fourier transform, where a $\cos^3$ window (having 10% width of the whole interval) is slid to span the time series containing 4×10^6 samples. The spectra shown are the result of averaging all the windows.

Figure 2 illustrates the good matching between the STAFF-SC and the FGM spectra at frequencies around 1.5 Hz. However, above $f \geq 2.5$ Hz, the power in the physical signal falls below the noise floor of the instrument, so we use STAFF-SC data to analyze frequencies above $f \geq 2.5$ Hz. Here we merge the low frequency FGM data with the STAFF-SC data at $f = 1.5$ Hz. Figure 2 shows a spectral breakpoint at $f \sim 0.4$ Hz where the scaling changes from a Kolmogorov spectrum $f^{-1.62}$ to

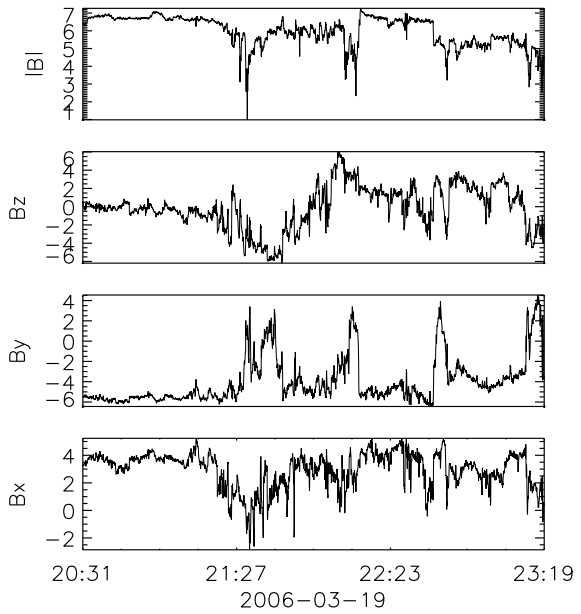

FIG. 1: FGM magnetic field data measured by Cluster 2 in the solar wind plotted in the Geocentric Solar Ecliptic (GSE) reference frame. The vertical dotted lines delimit two sub-intervals of time discussed in the text.

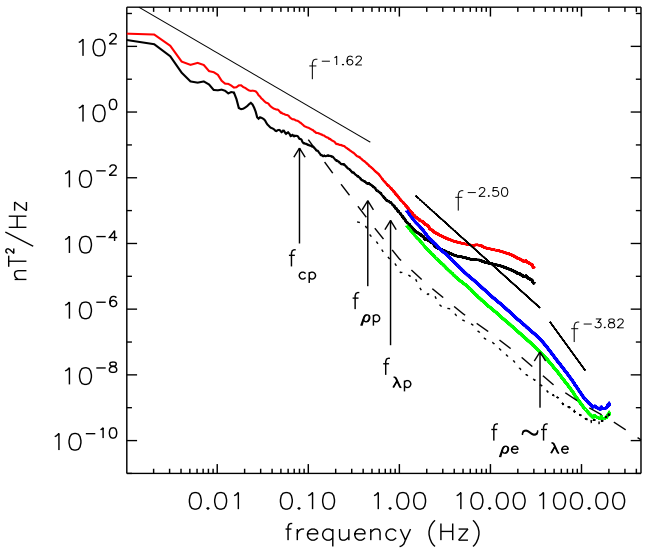

FIG. 2: The parallel (black) and perpendicular (red) magnetic spectra of FGM data ($f < 33$ Hz) and STAFF-SC data (respectively, green and blue; $1.5 < f < 225$ Hz). The STAFF-SC noise level as measured in the laboratory and in-flight are plotted as dashed and dotted lines, respectively. The straight black lines are power law fits to the spectra. The arrows indicate characteristic frequencies defined in the text.

$f^{-2.5}$. Similar breakpoints and steep spectra have been reported previously [5–8, 21], but mostly attributed to energy dissipation [5, 6]. The spectra of Figure 2 suggest rather a very different scenario: the magnetic energy continues cascading for about two decades higher in spacecraft frequency and smaller spatial scales. Furthermore, it shows the first evidence of a second breakpoint at $f \sim 35$ Hz, followed by a steeper spectrum of $f^{-3.9}$. To understand the origin of these breakpoints, we calculated the characteristic scales of the plasma, namely the proton and electron gyroscales and inertial lengths defined as $\rho_{p,e} = V_{th_{p,e}}/\omega_{cp,e}$, $\lambda_{p,e} = V_{A_{p,e}}/\omega_{cp,e}$, where V_{th} and V_A are the thermal and the Alfvén velocities, and $\omega_{cp,e}$ are the proton and electron gyrofrequencies. Using the Taylor frozen-in-flow hypothesis ($\omega \sim kv$) these scales are Doppler-shifted and represented in Figure 2. The Doppler-shifted proton and electron gyroscales fit better with the observed breakpoints than do the proton and electron gyrofrequencies (as has been suggested [6, 8]). In particular, the ratio of the two frequencies $35/0.4 \sim 90$ is very close to the ratio $\rho_p/\rho_e = \sqrt{m_p T_p/m_e T_e} \sim 95$.

The new breakpoint occurs at the electron gyroscale ρ_e, which is very close to λ_e (because $\beta_e \sim 1$). This can be seen clearly on Figure 3, which shows the high frequency part of two spectra calculated from sub-intervals of Figure 1 to investigate whether the foreshock electrons have a significant impact on the properties of the observed spectra. Spectra of Figure 3(a) were obtained in a an interval where electron foreshock were detected, whereas those of Figure 3(b) were calculated when no significant reflected electron were observed from the WHisper data (not shown here). Both spectra look very similar to those of Figure 2. This is not surprising since the population of electron foreshock represented only a few percents of the total SW electrons. Moreover, if the reflected electrons were to have any impact on the spectra, then this would result in strong spikes on the spectra at electrons scales/frequencies (as these electrons would inject additional energy into the turbulence). Here we observe rather a formation of steep dissipation-like spectum.

To investigate the nature of the small scale turbulence (i.e., above f_{ρ_p}) we computed the spectrum of the electric field component E_y (shown in Figure 4). Below f_{ρ_p} the spectrum of E_y shows a high correlation with the spectrum of B_z, and both follow a Kolmogorov scaling. For frequencies around f_{ρ_p} the E_y spectrum steepens slightly up to $f \sim 1.5$ Hz, where it becomes essentially flat. A fit of the spectrum in the interval $f \sim [1.5, 15]$ Hz shows a power law $\sim f^{-0.3}$. It is worth recalling here that GK theories predict the power laws ${k_\perp}^{-7/3}$ for the magnetic field spectrum and ${k_\perp}^{-1/3}$ for the electric field spectrum at these sub-proton gyroscales [16, 17]. The fact that the electric field spectrum continues with a nearly zero spectral slope above $f \geq 10$ Hz is due to reaching the noise level of the EFW experiment.

The present observations suggest that the energy of the turbulence is only slightly damped at the proton gyroscale ρ_p and undergoes another dispersive cascade with the scaling $f^{-2.3}$. Any strong damping would have led to a much steeper spectrum, if not to a clear cut-off [9]. Steepening of spectra (e.g., from $k^{-5/3}$ to $k^{-7/3}$) below the proton scale can indeed be explained solely by dispersive effects as has been predicted by various non-

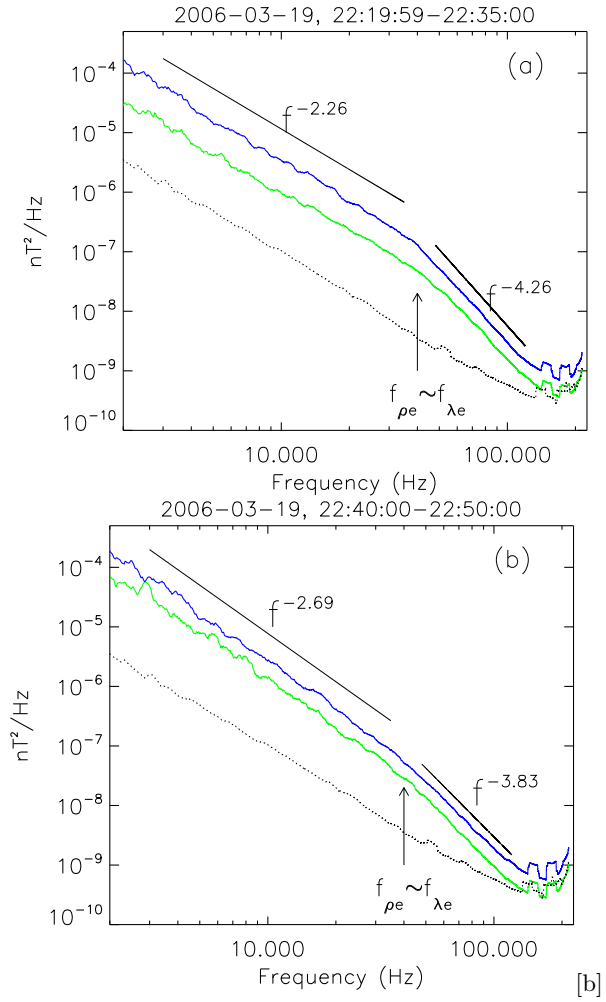

FIG. 3: High-pass filtered power spectra of the parallel (green) and perpendicular (blue) of the magnetic fluctuations measured by STAFF-SC during two time sub-intervals with beams of reflected electrons from the bow shock (a) and a nearly free solar wind (no significant reflected electrons) (b). Dotted line is the STAFF-SC noise level. The straight black lines are direct power law fits of the spectra. Vertical arrows are defined in the text.

dissipative dispersive MHD models [11, 12, 22, 23]. However, as we show below, finite dissipation may occur at the proton scale ρ_p along with more significant damping at the electron gyroscale ρ_e. This latter may explain the stronger steepening of the spectrum to f^{-4} (the power law fits in the dissipation range may be not very accurate because they extended over less than a decade due to the noise level of the instrument).

III. THEORETICAL INTERPRETATION: 2-D KAW TURBULENCE CASCADE

This scenario of dispersive cascade and dissipation at electron scales appears consistent with Kinetic Alfvén Wave (KAW) turbulence as predicted by the GK theory [16, 17]. The predicted scalings $B^2 \sim {k_\perp}^{-7/3}$ and $E^2 \sim {k_\perp}^{-1/3}$ are in striking agreement with these observations. KAW turbulence has been observed previously [10, 24], but only at large (proton) scales (up to 10 Hz). Here we are observing KAW behavior down to electron scales where enhanced dissipation becomes evident. This can be explained by electron Landau damping, as it is shown below.

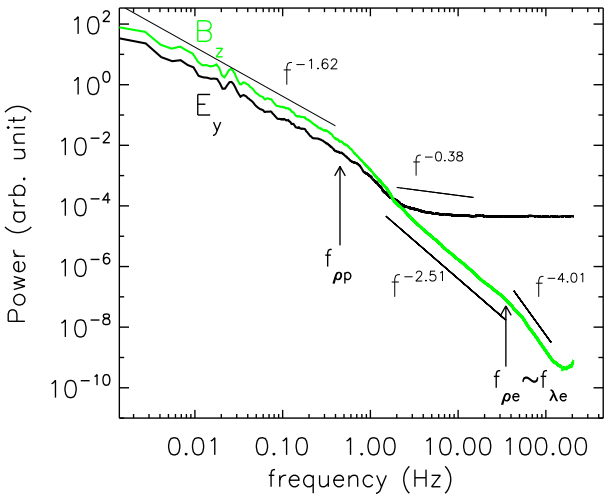

FIG. 4: Spectra of data from spacecraft 4 in the Despun System of reference (DS): E_y measured by EFW (bold black curve) and B_z measured by FGM and STAFF-SC merged at 1.5 Hz (green). The straight black lines are direct power law fits of the spectra. Vertical arrows are the Doppler-shifted proton and electron gyroradius and inertial lengths.

To confirm this scenario of KAW energy cascade and dissipation, we have solved numerically the Maxwell-Vlasov equations [25] assuming Maxwellian distributions of protons and electrons with characteristics that reflect the physical parameters deduced from the data. We assumed that the turbulence was quasi-two-dimensional (2D), i.e., $k_\parallel << k_\perp$. This assumption is justified by an analysis (not shown here) that used the k-filtering technique on the **k**-vectors distribution at large scales ($f < 10^{-2}$ Hz). That analysis confirmed the 2D nature at large scales. This 2D picture at large scales is likely to continue at the small scales as reported in previous studies [24, 26]. Several previous observations have also reported the dominance of the 2D turbulence in the SW [23, 27].

The results shown in Figure 5 prove that under the plasma conditions observed here, KAW can propagate over a wide range of scales before being damped at the electron gyroscale [9, 13]. The mode is shown to be only slightly damped at $k\rho_p \sim 1$ where $|\gamma|/\omega_r \sim 0.1$ (γ is the damping rate and ω_r is the real part of the frequency). The KAW mode is however strongly damped by electron Landau resonance at $k\rho_e \sim 1$ where $|\gamma|/\omega_r \sim 1$, which may explain the steepening of the magnetic spectrum to f^{-4} (here the resonance con-

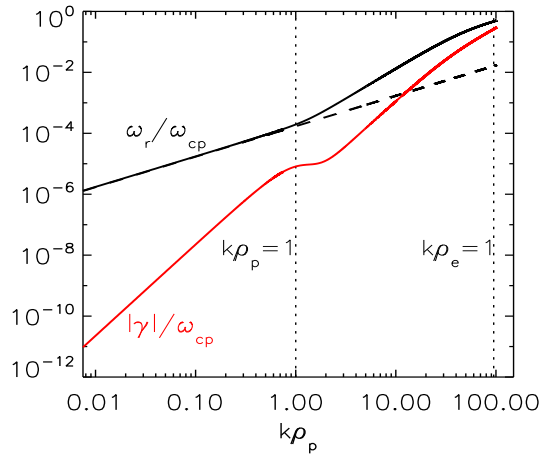

FIG. 5: Linear solutions of the Maxwell-Vlasov equations for $\theta = \arccos(\mathbf{k}, \mathbf{B_0}) = 89°$, obtained using the plasma parameters given in the text. The real part of the frequency (black) and the damping rate (red) are consistent with the kinetic Alfvén wave dispersion relation and damping [9, 16]. The dashed line is the asymptote $\omega/\omega_{cp} = k_\parallel V_A/\omega_{cp}$. The plots stop at scales where $|\gamma| \sim \omega_r$.

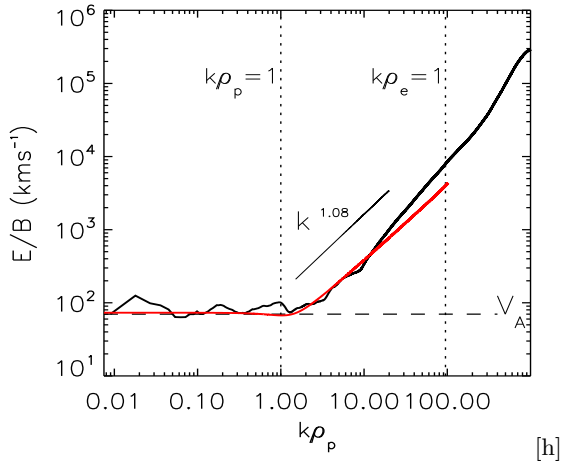

[h]

FIG. 6: The ratio E_y/B_z measured by Cluster 4 (black) compared to a similar ratio calculated from the linear Maxwell-Vlasov theory (red). The electric field data have been transformed into the plasma reference frame using the Lorentz transform $\mathbf{E}_{plas} = \mathbf{E}_{sat} - \mathbf{VxB}$ [10]. The horizontal dashed line is the Alfvén speed. The straight black line is a direct fit of E_y/B_z from $k\rho_p = 1.5$ to $k\rho_p = 20$. We used $\theta = \arccos(\mathbf{k}, \mathbf{v}) = 50°$ to transform frequency to $k\rho_p$.

dition $\omega_r \sim k_\parallel V_{th_e}$ and the KAW dispersion relation $\omega_r = \pm k_\parallel V_A k_\perp \rho_p / \sqrt{\beta_p + 2/(1+T_e/T_p)}$ [17] yield the dissipation scale $k\rho_e \sim 0.8$). We notice however that for moderate oblique propagation angles $\leq 80°$, scales $k\rho_p > 15$ are damped by proton Landau/cyclotron resonance ($\omega_r \sim \omega_{cp}$), which may yield proton heating.

Figure 6 shows a comparison between the ratio of the electric to the magnetic field measured by Cluster and calculated from the linear kinetic theory of the KAW.

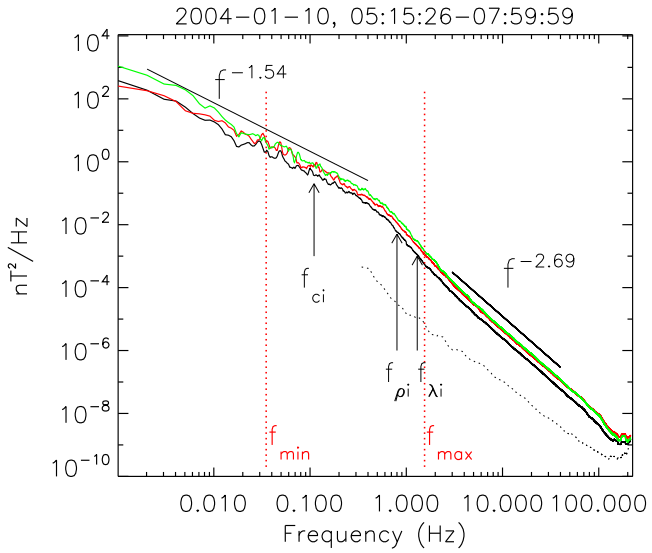

FIG. 7: Merged spectra from FGM ($f < 1.5$ Hz) and STAFF-SC data ($1.5 < f < 225$ Hz) in GSE on 20040110 from 06h05 to 06h55. The vertical dotted lines (red) limit the range of frequencies accessible to analysis using the k-filtering [21]. The same description as in Figure 2 applies to the rest of the figure.

There is very good agreement between theory and observations: (i) At large scales ($k\rho_p \leq 1$) the similar scaling $E^2 \sim B^2 \sim k^{-1.62}$ yields a constant ratio $V_\phi = E/B \sim V_A$, in agreement with the frozen-in flow approximation $\mathbf{E} = -\mathbf{V} \times \mathbf{B}$; (ii) At the scale $k\rho_p \geq 1$, dispersive effects set in yielding the linear scaling of the phase speed $V_\phi \sim k^{1.08}$, which also agrees with GK theory because $E^2/B^2 \sim {k_\perp}^2 \Rightarrow V_\phi \sim k_\perp$. We note finally that the departure from this linear scaling observed in Figure 6 for $k\rho_p > 20$ is due to the noise in the electric field data that causes the flat E_y spectrum mentioned above. One would expect to observe a steepening of the E_y spectrum similar to B_z when the dissipation scale $k\rho_e \sim 1$ is reached [17].

IV. MULTI-SPACECRAFT ANALYSIS OF SUB-PROTON SCALES USING THE *K*-FILTERING TECHNIQUE

The results shown above were obtained in a time interval where the Cluster spacecraft were separated by about 1000 km. These large spacecraft separation preclude using the k-filtering method to estimate the 3-D wavenumber spectra and, consequently, investigate the nature of the small scale turbulence of interest here [21, 28]. Therefore, we analyzed another data set where the spacecraft separation were about 100 km. The spectra of the magnetic turbulence are shown on Figure 7.

We can see on Figure 7 that the breakpoint at proton scales falls within the interval of frequencies $[f_{min}, f_{max}] = [0.04, 2]$ Hz accessible to analyzis using the k-filtering [21]. Applying the k-filtering method on

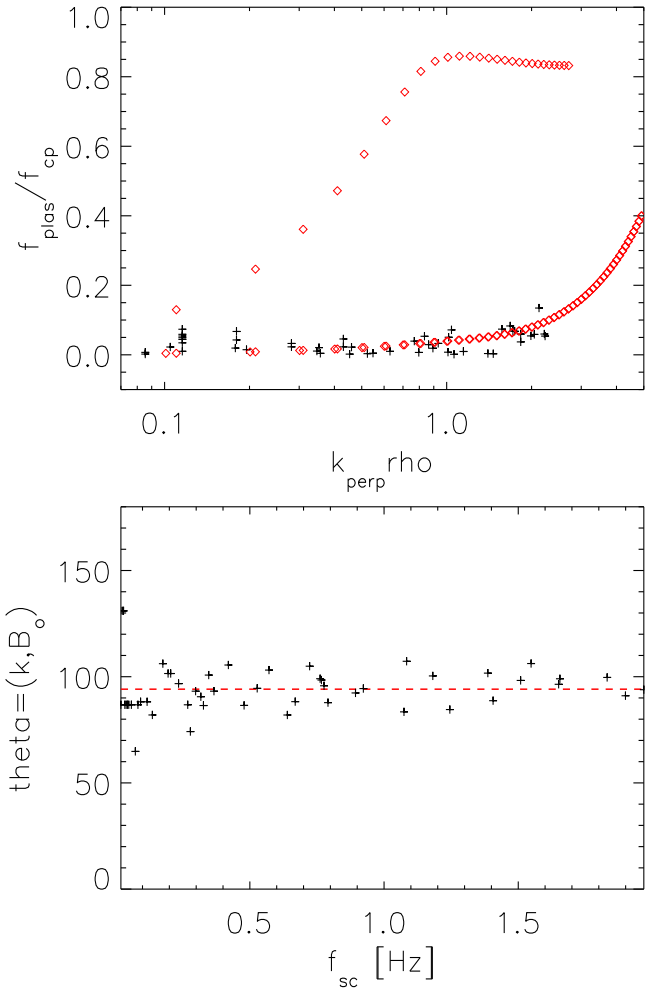

FIG. 8: Top: the angles between the local magnetic field and the **k**-vectors of the turbulence estimated using the *k*-filtering technique for the interval of frequencies depicted on Figure 7. Bottom: comparison of the experimental dispersion relations (black crosses) to the theoretical ones as computed from the linear Vlasov theory (red diamonds) for the average angle $\theta =< (\mathbf{k}, \mathbf{B}_0) >\sim 86°$ (dashed red line).

each frequency of this interval allowed us to obtain the 3-D **k**-spectra of the turbulence, resolving therefore its anisoptropy and nature at the corresponding scales (A more complete study of this interval will be published elsewhere).

As shown of Figure 8, we found that the **k**-vectors of the turbulence lie nearly in the plane perpendicular to the mean magnetic field, with a mean angle $\theta =< (\mathbf{k}, \mathbf{B}_0) >\sim 86°$. It is worth noting that this result is valid both below and above the proton gyroscale. This result validates the assumption used in [29] that large (proton) scale anisoptropies "survive" at small (electron) scales. The bottom plot in Figure 8 compares the experimental dispersion relations to the theoretical ones as computed from the linear Vlasov theory for the observed angle $\theta =< (\mathbf{k}, \mathbf{B}_0) >\sim 86°$ and using the observed plasma parameters. This plot shows clearly that the turbulence is nearly stationary in the plasma rest frame ($f_{plas} << f_{cp}$ and follows the dispersion curve of the Alfvén mode $\omega \sim k_\parallel V_A$ up to the scale $k_\perp \rho \sim 2.5$. The observed experimental "dispersion" relations lie very far from the fast mode. Because larger **k**-vectors than the ones shown here are not accessible to measurements, we cannot conclude whether or not the nature turbulence at smaller scales (or higher frequencies) may change follow the whistler mode. We will discuss in more detail this problem in a forthcoming paper.

V. DISCUSSION AND CONCLUSIONS

We reviewed recent observations of cascade of the SW turbulence below the proton gyroscale and its dissipation at the electron gyroscale. We have shown that the kinetic theory of the highly oblique KAW turbulence can account for the observed cascade and dissipation. We found that collisionless electron Landau damping consistently explains the observations rather than proton cyclotron damping. These results were first obtained from mono-spacecraft analysis. Then they have been confirmed from direct multi-spacecraft measurements of the **k**-vectors of turbulence at sub-proton scales using the *k*-filtering method, when the Cluster separation were appropriate. This mechanism of cascade and dissipation at small scales may be applicable in other astrophysical contexts [7, 16]. For example, in the solar corona, electron Landau damping, as observed here, may be an efficient mechanism for heating electrons. An open question remains however which is related to the physical conditions under which one would observe either scenarii: i) a dissipation-like spectra at the proton scale; ii) a continuous cascade below the proton scale and dissipation at the electron scale. This problem is currently being investigated.

Acknowledgments

The FGM, PEACE and CIS data come from the CAA (ESA) and AMDA (CESR, France).

[1] C. P. Escoubet, *et al.*, *The Cluster and Phoenix Missions* (Kluwer Academic Publishers, Belgium, 1995).
[2] W. H. Matthaeus and M. L. Goldstein, J. Geophys. Res. **87**, 6011 (1982).
[3] F. Sahraoui and M. L. Goldstein, In preparation (2010).
[4] Y. Narita, *et al.*, Phys. Rev. Lett. p. submitted (2010).

[5] M. L. Goldstein, *et al.*, J. Geophys. Res. **99**, 11519 (1994).
[6] R. J. Leamon, *et al.*, J. Geophys. Res. **103**, 4775 (1998).
[7] R. J. Leamon, *et al.*, Astrophys. J **537**, 1054 (2000).
[8] O. Alexandrova, *et al.*, Astrophys. J **674**, 1153 (2008).
[9] O. Stawicki, *et al.*, J. Geophys. Res. **106**, 8273 (2001).
[10] S. D. Bale, *et al.*, Phys. Rev. Lett. **94**, 215002 (2005).
[11] D. Biskamp, *et al.*, Phys. Plasmas **6**, 751 (1999).
[12] V. Krishan and S. M. Mahajan, J. Geophys. Res. **109**, doi:10.1029/2004JA010496 (2004).
[13] S. P. Gary, *et al.*, Geophy. Res. Lett. **35**, L02104 (2008).
[14] S. Galtier, J. Plasmas Phys. **72**, 721 (2006).
[15] F. Sahraoui, *et al.*, J. Plasmas Phys. **73**, 723 (2007).
[16] A. Schekochihin, *et al.*, Astrophys. J. **182**, 310 (2009).
[17] G. G. Howes, *et al.*, Phys. Rev. Lett. **100**, 065004 (2008).
[18] A. Balogh, *et al.*, Ann. Geophys. **19**, 1207 (2001).
[19] N. Cornilleau, *et al.*, Ann. Geophys. **21**, 437 (2003).
[20] G. Gustafsson, *et al.*, Ann. Geophys. **19**, 1219 (2001).
[21] F. Sahraoui, *et al.*, Planat. Space Phys. p. submitted (2009).
[22] S. Galtier, Phys. Rev. E **77**, 015302 (2008).
[23] W. Matthaeus, *et al.*, J. Geophys. Res. **95**, 20673 (1990).
[24] B. Grison, *et al.*, Ann. Geophys. **23**, 3699 (2005).
[25] K. Ronmark, *Report 179 of Kiruna Geophys. Inst.* (Kiruna Geophysical Institute, Sweden, 1982).
[26] F. Sahraoui, *et al.*, Phys. Rev. Lett. **96**, 075002 (2006).
[27] T. Osman and T. Horbury, Astrophys. J **654**, L103 (2007).
[28] F. Sahraoui, *et al.*, J. Geophys. Res. p. in press (2009).
[29] F. Sahraoui, *et al.*, Phys. Rev. Lett. **102**, 231102 (2009).